JOURNAL OF GEOPHYSICAL RESEARCH, VOL. 98, NO. D7, PAGES 12,881–12,893, JULY 20, 1993

Convective Cloud Systems and Warm-Pool Sea Surface Temperatures: Coupled Interactions and Self-Regulation

DUANE E. WALISER

Department of Atmospheric Sciences, University of California, Los Angeles

NICHOLAS E. GRAHAM

Climate Research Division, Scripps Institution of Oceanography, University of California, San Diego, La Jolla

Questions regarding the upper limits on tropical sea surface temperatures and the processes determining those limits have recently come under renewed interest and debate. We present results from an analysis of the relationship between observed sea surface temperature (SST) and organized deep convection in the tropics that has produced new and important findings relevant to this issue. First, the analysis reveals that the highest observed tropical SSTs are generally associated with diminished convection. Second, the maximum convective activity occurs, on average, at an SST of about 29.5°C. Third, at SSTs of about 29°C and greater, intense deep convection is associated with ocean surface cooling of approximately 0.1°C per month, while suppressed deep convection is associated with a similar degree of ocean surface warming. These three findings, together with results from simplified model analyses, emphasize the importance of the cooling mechanisms associated with deep convection in determining the observed upper limits on tropical SST. Implications of the observed relationship between deep convection and SST on the temporal correlations between these fields is discussed, as is the convective cloud system's relative influence on the solar and evaporative heat flux components of the surface energy budget.

1. INTRODUCTION

The processes controlling the Earth's surface temperature are central to defining climate and determining the character of climate change. The role these processes play in regard to the oceanic component of the climate system is of particular importance because of the ocean's ability to absorb, retain and transfer heat over the globe and because the ocean represents the dominant heat source for the Earth's troposphere. The connection between ocean surface temperatures and climate is particularly pronounced in the tropics where organized deep convective systems act to transfer heat and moisture from the ocean via the atmospheric boundary layer into the free atmosphere. In simplified terms, these convective systems are composed of three structures: (1) narrow ascent regions ($<\sim 10^2$ km^2) of deep cumulonimbus clouds and intense precipitation that produce net heating over nearly the entire tropospheric column; (2) a larger region (10^2–10^4 km^2) of precipitating mid- to high-level stratiform cloud that produces net heating in the upper troposphere and net cooling the lower troposphere; and (3) a much larger (10^4–10^6 km^2) region of cirrus clouds near the tropopause [*Leary and Houze*, 1979; *Houze*, 1989; *Liou*, 1986]. The latent heat released in the higher levels of these organized convective systems has a profound effect on the global atmospheric circulation. In addition, the clouds associated with these systems contribute importantly to the albedo and thus to the surface energy balance. Considered collectively, organized deep convective systems act to stabilize the tropical troposphere which is heated and supplied with moisture from the ocean surface below (via turbulent surface fluxes), by cooling and drying the lower levels and warming and moistening the upper levels.

The relationship between sea surface temperature (SST) and large-scale convective systems has been studied in a variety of contexts for several decades [e.g., *Bjerknes*, 1966; *Webster*, 1972; *Lindzen and Nigam*, 1987; *Neelin and Held*, 1987; *Zhang*, 1993]. Most often, these studies have been concerned with the role ocean surface temperatures play in forcing atmospheric convection. One important aspect of the character of deep convection revealed through such studies is that it generally occurs more frequently and/or with more intensity as SSTs become higher, with a particularly sharp increase when SSTs exceed 27°–28°C [*Krueger and Gray*, 1969; *Gadgil et al.*, 1984; *Graham and Barnett*, 1987]. The questions of whether and how such a value behaves as a "threshold" for the organization of such systems has fostered considerable interest [e.g., *Lau and Shen*, 1988; *Betts and Ridgway*, 1989]. These studies suggest that this surface temperature approximates the value at which the vertical stability of the tropical troposphere is sufficiently reduced to allow the onset of large-scale moist convection.

Another important but less well known characteristic of the relationship between SST and deep convection is that at temperatures above about 29.5°C, the amount/intensity of convection observed tends to decrease with increasing SST [*Waliser et al.*, 1993]. This behavior contrasts with that described above where the inference is that increased SST results in increased convection. Here the suggestion is that very warm SSTs may only occur under conditions of diminished convection, thus indicating that convection acts to decrease (and possibly limit) sea surface temperatures. Such decreases (or limitations) can result from (1) reductions in the incoming solar radiation due to the associated cloud systems, and/or (2) enhancements to surface fluxes of heat and moisture out of the ocean surface due to the vertical

Paper number 93JD00872.
0148-0227/93/93JD-00872$05.00

overturning associated with deep convection. Many early studies have examined the role convective exchange of heat and moisture plays in maintaining the vertical temperature profile of the Earth's atmosphere (including the surface temperature), mostly in the context of radiative-convective models of the atmosphere [e.g., *Manabe and Weatherald*, 1967; *Ramanathan and Coakley*, 1978].

Considerations of the role that cloud processes play in placing a natural limit on SST, however, have been less common, and have most often been posed in terms of their role in a changing climate, such as in the possible warming resulting from increased CO_2 [e.g., *Paltridge*, 1980; *Somerville and Remer*, 1984; *Lindzen*, 1990; *Arking*, 1991]. One simplified account of the role clouds may play in determining the "upper limit" on SSTs was given by *Graham and Barnett* [1987]. Their analysis of the relationship between SST and convection, along with results from an idealized surface heat budget model [cf. *Newell*, 1979], led them to suggest that the cloud cover associated with organized deep convection may act to limit SSTs through a reduction of surface insolation. Using satellite-derived radiation budget estimates, *Ramanathan and Collins* [1991, 1992] found evidence of a "super greenhouse" effect at the upper range of observed SSTs. This effect increasingly limits the amount of longwave cooling to space as SSTs rise, potentially leading to an uncontrolled warming. They hypothesized that highly reflective cirrus clouds (resulting from the atmospheric convection associated with increased SSTs) act as a "thermostat" limiting further increases in surface temperature. This hypothesis has been questioned by *Wallace* [1992], who argues conceptually that cloud forcing does not play an important role in regulating "warm-pool" surface temperatures on a local scale, and by *Fu et al.* [1992], who examine the evidence for such a regulating mechanism when considering the nonlocally coincident relation between convection and SST averaged over large spatial scales.

In this paper we consider the local relationships between SST and estimates of organized deep convection to infer the role convection plays in limiting ocean surface temperatures. First, we present findings and analyses that provide strong observational evidence that the cooling mechanisms associated with organized deep convection act to limit tropical SSTs to values of about 29.0°C. Next, we present a conceptualized model of three interacting processes within the coupled ocean and atmosphere system to explain the observed relationships between SST and deep convection. We then incorporate these processes into a simplified energy balance model to demonstrate that these processes can qualitatively reproduce many aspects of the observed relationships. Last, we summarize the results and their implications, emphasizing the role of interactions between organized convection, cloud albedo, evaporative heat flux, and SSTs in determining the character of the ocean/atmosphere system in the warm pool regions of the tropics.

2. DATA

Three principal data sets were used in the analysis, outgoing longwave radiation (OLR), highly reflective cloud (HRC), and SST. OLR is an estimate of the total outgoing infrared (IR) radiation at the top of the atmosphere inferred from multiband satellite radiation measurements [*Gruber and Krueger*, 1984]. It has been used in many studies as an indicator of deep convection over tropical oceans [e.g., *Liebmann and Hartmann*, 1982; *Rasmusson and Wallace*, 1983; *Graham and Barnett*, 1987]. Its use for this purpose is based on the fact that from space the upwelling thermal radiation appears to radiate from a virtual surface corresponding to the highest water surface (vapor, liquid, ice) in the atmospheric-ocean column. In the presence of clouds, this surface corresponds to the highest cloud top, while in cloud-free conditions, this surface is located in the lower to mid-troposphere, typically about 3–5 km. (In clear conditions, the signal is an integrated measure of the surface signal through, and emitted by, the vertical distribution of water vapor, which mainly occurs in the lowest 2–4 km. This signal is easily distinguished from that emitted from convective cloud tops rising to 10–14 km.) The amplitude of the emitted radiation is a function of the temperature of the virtual surface (roughly σT^4), which in turn is mainly a function of its altitude. Since temperature typically decreases with height in the troposphere, low-OLR values indicate the presence of high cloud tops (an attribute of deep convection), and high OLR values imply low clouds or clear conditions. The principal disadvantages in using OLR as a proxy for deep convection [*Waliser et al.*, 1993] are (1) OLR is a based on IR data only and thus cannot distinguish between the cirrus clouds and the precipitating elements of a convective system, (2) time-averaged OLR is a convolution of the radiative effects of the cloud and water vapor fields; the close relation between the latter and the underlying SST [*Stephens*, 1990] can result in biased estimates of deep convection (For example, one cloudy day and one clear day occurring over warm water will produce a different value than the same conditions occurring over cooler water.), and (3) difficulties result from changes in local (diurnal) satellite crossing time [*Chelliah and Arkin*, 1992; *Gadgil et al.*, 1992]. In original form these data are available as daily daytime and nighttime values with a spatial resolution of approximately 100 km. The monthly and 5-day OLR data used here were constructed by *Horel and Cornejo-Garrido* [1986].

HRC [*Garcia*, 1985] is a binary indicator of the presence of organized deep convection based on the subjective analysis of daily visible and IR satellite mosaics (daytime only). As in the case of OLR, the IR data are used as a proxy for cloud top height and thus to indicate the presence of high clouds. The visible information is used to exclude the large-scale cirrus clouds associated with convective systems. In addition, the visible data provide critical information over tropical land masses and in other regions and conditions (e.g., low SST) where interpretations from infrared data only are inconclusive. The results from this analysis are combined in the form of binary-valued "images" with 1° spatial resolution that indicate regions where large-scale convection is present. The principal disadvantages of the HRC [*Waliser et al.*, 1993] are (1) its determination is subjective, (2) in raw (daily) form it is a binary measure, that is, convection or no convection at each grid point, (3) it is measured only once per day, and (4) as with OLR, it is also sensitive to changes in local satellite crossing time. In contrast to OLR, HRC has the distinct advantage that it is designed to be insensitive to SST, atmospheric water vapor, and the presence of thin cirrus and other clouds not associated with organized convection.

The SST data combine an in situ measurement analysis from 1975–1981 with a blended analysis of satellite-derived

and in situ measurements from 1982–1987, each produced monthly on a 2° × 2° grid [*Reynolds*, 1988]. For the analyses described here, the OLR and HRC data were processed to provide monthly values (Wm^{-2} and days/month, respectively) on the same 2° × 2° grid between 25°N and 25°S for the period 1975–1987.

Additional data sets include the monthly Florida State University surface wind data set from the years 1975–1987 [*Legler and O'Brien*, 1984] and a 6-year record of integrated atmospheric water vapor (w) retrievals from satellite-based microwave instruments. The retrievals of w were obtained from the scanning multichannel microwave radiometer instrument for the years 1980–1982 [*Liu*, 1989] and from the TIROS operational vertical sounder instrument for the years 1983–1985 [*Rossow and Schiffer*, 1991]. Each of the above data sets was mapped to the grid described above. The water vapor retrievals were used to compute the monthly mean specific humidity of the near-surface layer (q_a) using the method of *Liu* [1986] which has a reported rms accuracy of less than 0.8 g/kg over most global oceans when compared against in situ data. These q_a values were then used to compute the difference between the saturation specific humidity at the surface temperature and the near-surface specific humidity ($\Delta q = q_s(\mathrm{SST}) - q_a$), a term important in the determination of the ocean surface evaporative heat flux. Hourly surface-measured solar irradiance data from American Samoa [*Dutton*, 1992], covering the period 1976–1987, were averaged into 5-day means for direct comparison with coincidental 5-day HRC and OLR data.

3. Local Relationships Between SST and Deep Convection

Figure 1 shows mean HRC (Figures 1*a* and 1*c*) and OLR (Figure 1*b*) for 0.5°C SST bins plotted as a function of SST for the global tropical oceans [cf. *Graham and Barnett*, 1987; *Waliser et al.*, 1993]. The standard deviations of the means and the number of observations in each bin are also plotted. The HRC and OLR curves in Figures 1*a* and 1*b* were computed using monthly SST and convection indice data. These two curves are quite similar; each indicates that the intensity (or frequency) of organized convection rises sharply as SSTs increase from 26.5° to 29.0°C, reaches a maximum at 29.5°C, and then declines at higher temperatures. As mentioned earlier, the ascending branch of this relationship has been the subject of considerable research. The sharpness of the increase is thought to reflect the fact that the typical vertical moisture and temperature structure of the atmosphere over the tropical oceans is such that large-scale surface temperatures above about 27°–28°C are required to provide the necessary moist static energy to the near-surface layers in order for saturated air parcels to ascend into the high troposphere, that is, for deep convection to occur [e.g., *Lau and Shen*, 1988; *Betts and Ridgway*, 1989]. If this process alone were operating, one might expect convection to increase, or remain at some maximum, at very high SSTs. However, the two curves show that for SSTs above 29.5°C, organized convection decreases as SST increases. There is little reason to believe this tendency for decreased convection with increased SST is an artifact. First, the fact that two quite different convection proxies give nearly identical results argues against this possibility. Second, despite the relatively small sample sizes at higher

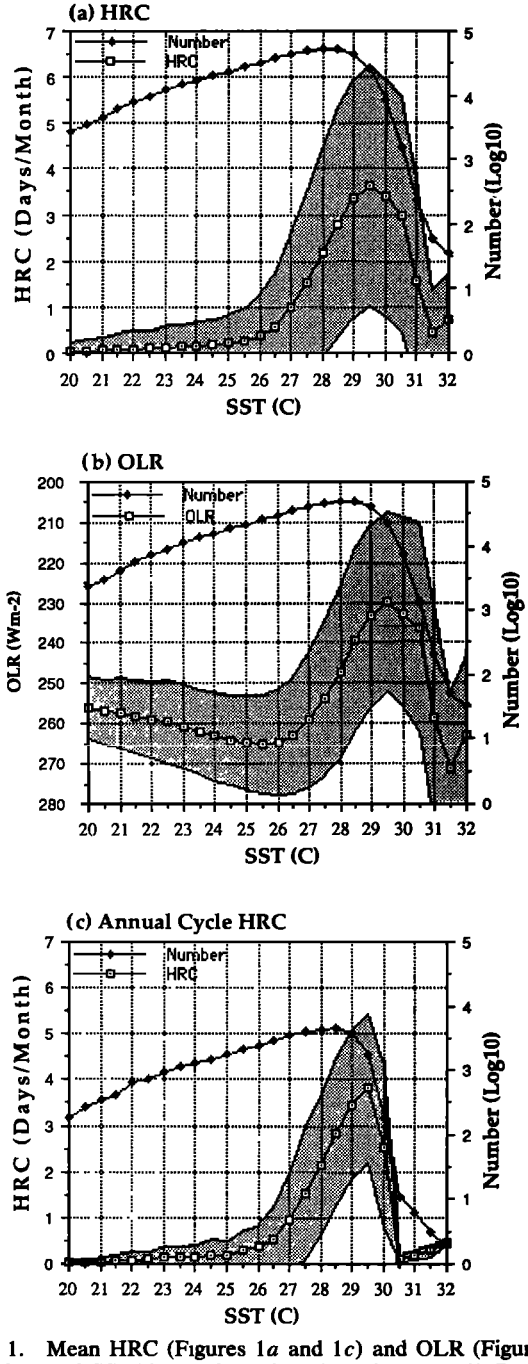

Fig. 1. Mean HRC (Figures 1*a* and 1*c*) and OLR (Figure 1*b*) values for 0.5°C SST bins. Values plotted are the mean HRC or OLR for all cases of a given SST bin between 1975–1987 for the global tropical oceans between 25°N and 25°S. (*a*) and (*b*) Plots are computed from monthly convective indice and SST values. (*c*) Plot is computed from 12-month mean annual cycle data. The number of values (line with circles) used in the computation of the means is specified by the right vertical axes. The standard deviation of the means are delineated by the shading. Note the OLR axis in Figure 1*b* is reversed for easier comparison with the HRC.

SSTs, statistical tests (t test for 99% confidence interval) support the inference that adjacent OLR and HRC bin means at SSTs of 29.5°C and above are distinct (except the pair at 31.5° and 32.0°C).

The results shown in Figures 1*a* and 1*b* indicate that very little organized convection occurs in association with SSTs above about 30.5°C. This suggests that the suppression of

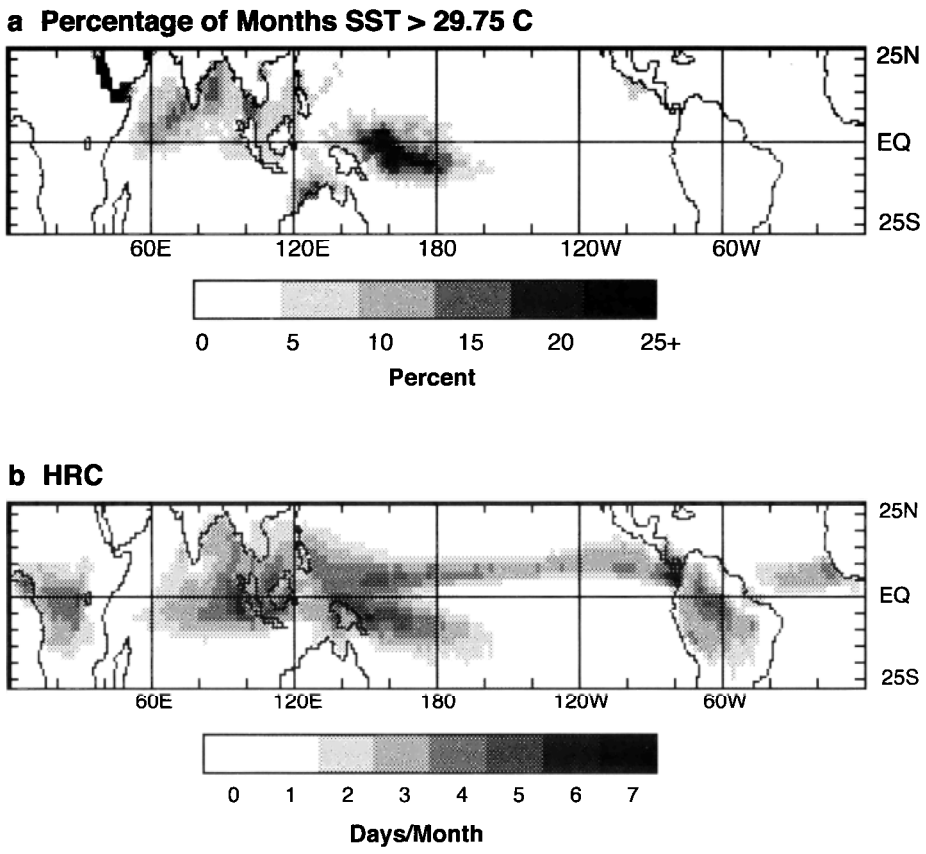

Fig. 2. (*a*) Fraction of monthly SST values greater than 29.75°C and (*b*) mean monthly HRC for the study period 1975–1987 (156 months).

organized convection is an important factor in allowing these unusually warm temperatures to be achieved, or alternatively, that the presence of organized convection tends to limit upward excursions of SSTs. Because this premise is of considerable climatological importance and is inferred above only on the basis of monthly data composited over the global tropical oceans, below we consider the relation between organized convection and SSTs from a variety of temporal and spatial perspectives. For example, the plot in Figure 1*c* is analogous to Figure 1*a* but was produced from long-term mean annual cycle data and is used here to represent "equilibrium" conditions. Figure 1*c* emphasizes two key characteristics of the relation between organized convection and SSTs inferred from Figures 1*a* and 1*b*. First, the extreme rarity of SSTs above 29.5°C, along with their greater relative reduction in number as SST increases as compared to Figure 1, suggests that within the coupled system (as presently constituted), large regions with SST higher than about 29.5°C cannot be maintained in equilibrium given the negative feedbacks of organized convection on SST warming. Second, Figure 1 demonstrates that in the rare instances long-term average SST observations are above 29.5°C, they exist only under conditions of diminished convection (regions where the large-scale circulation is likely acting to suppress deep convection). Further support for the generality of the high SST-low convection association comes from plots (not shown) of HRC and OLR anomalies versus SST. These plots show that, in addition to being associated with diminished total convection (e.g., Figure 1), SSTs above about 30°C tend to be associated with negative convection anomalies as well.

To consider the organized convection-SST relation in spatial terms, Figure 2 shows maps of the fraction of months the SST was above 29.75°C (Figure 2*a*) and of the average HRC (Figure 2*b*) for the 13-month study period. SST bins are every 0.5°C. Thus the values in the 29.5°C bin range between 29.25–29.75°C. Therefore, Figure 2 maps SSTs greater than 29.75, that is, the observations that make up the bin means above the 29.5°C bin. The OLR equivalent of Figure 2*b* is qualitatively the same [*Waliser et al.*, 1993]. While not showing contemporaneous values of SST and convection (as in the plots in Figure 1), these maps are presented here to illustrate that although very warm SSTs are commonly observed in regions where convection is suppressed (e.g., the Arabian Sea, and off northwestern Australia), they also occur frequently in regions where organized convection is common (e.g., the western Pacific "warm pool"). The generality of the high SST-low convection relation is also addressed by the plots in Figure 3 which are analogous to those of Figures 1*a* and 1*b* but were constructed using data from the warm pool region of the western Pacific only. These HRC (Figure 3*a*) and OLR (Figure 3*b*) curves show the same qualitative features as those for the global tropics (Figures 1*a* and 1*b*), although they exhibit a more modest reduction in convection at high SSTs. As discussed below, such a difference might be expected. The above results demonstrate that the local association between very warm (monthly or longer-term

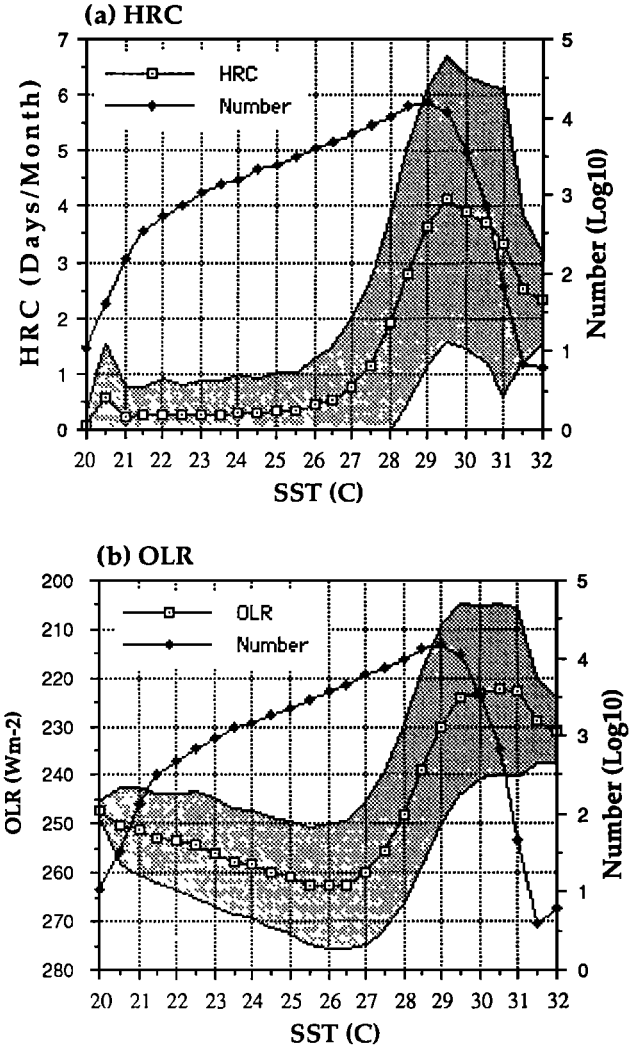

Fig. 3. The same as Figures 1*a* and 1*b* except that the longitude domain is restricted to the range 140°E to 170°W.

average) SSTs and diminished or low amounts of organized convection does not appear to be dependent on any particular climatological setting.

As noted earlier, previous research has provided some understanding of the mechanisms responsible for the character of the positive relationship between SSTs and organized convection at SSTs below about 29.5°C; in this range, the dominant forcing relation is of increased SSTs promoting the development of organized convection. Our analysis focuses on the mechanisms responsible for the character of the negative relationship between SSTs and convection at SSTs above 29.5°C; that is, where we suspect an equally important forcing relation of increased organized convection inhibiting further increases in SSTs. Clearly, the negative correlation between SSTs and organized convection at higher temperatures (>29.5°C) cannot be explained by the mechanisms associated with the positive correlation at lower temperatures (<29.5°C). One difficulty in exploring the relation between SST and convection at high SSTs is that if the observed behavior is due to the cooling mechanisms associated with organized convection (e.g., cloud cover), it is not immediately clear whether the more apparent relation should be between decreased convection and high SST, or whether it should be between decreased convection and positive rates of change of SST with time ($d\mathrm{SST}/dt$). To address this question and highlight some of the important physical parameters involved, we consider a very simple energy balance model of an idealized oceanic "mixed layer." The time evolution of the model mixed-layer temperature (i.e., surface temperature) is governed by three processes: (1) heating due to surface insolation; (2) cooling due to surface evaporation; and (3) an independently fluctuating "convection" component, chosen here as a modulation to the surface insolation (hereafter referred to as "cloud"). Formally, the system is given by

$$\frac{d\mathrm{SST}}{dt} = \frac{1}{c_p \rho_w H}\{I_o[1 - C \sin(\omega t)] - L\rho_a C_D U[q_s(\mathrm{SST}) - q_a(T_a)]\} \quad (1)$$

where H is the depth of the mixed layer, U is the near-surface wind speed, ω and C are the cloud forcing frequency and amplitude, I_o is the specified mean surface insolation, L is the latent heat of vaporization, C_D is the turbulent exchange coefficient; q_a, ρ_a and T_a are the specific humidity, density, and temperature in the near surface atmospheric layer; q_s, ρ_w and c_p are the saturation specific humidity, seawater density, and specific heat capacity at the mixed-layer temperature. While this simple model ignores many processes such as thermal radiation, ocean mixing, and advection, coupling between the wind and the "clouds," and the role SST plays in forcing the "clouds" (C), it does incorporate the two dominant processes determining the tropical surface heat budget and suffices to demonstrate important aspects of the expected relationship between SST, its time derivative, and convection for the range of very high SSTs.

For the purposes of obtaining an analytical solution, we assume fixed values of 27.5°C and 80% for the near surface air temperature and relative humidity, respectively, then linearize the Δq term of the evaporative flux. The slope of this linearization is important because in this formulation it provides the strength of the restoring force which acts to oppose changes in SST. Figure 4 shows that in the range of high SST (>~29°C), such an approximation yields values of Δq that agree well with satellite-derived observations from the warm-pool region (similar agreement is found when comparing against in situ data). The solution to the linearized equation gives the temperature evolution of our idealized ocean "mixed layer" as a function of mixed-layer depth, surface wind speed, cloud forcing frequency, and amplitude, and β (representing the strength of the restoring force):

$$\mathrm{SST}(t) = \left\{T_o - \frac{(DC/H\omega)}{[(\beta U/H\omega)^2 + 1]} \sin(\omega t + \phi)\right\} \quad (2)$$

where $\phi = a\tan(-H\omega/\beta U)$, $q_s(\mathrm{SST}) - q_a(T_a) \cong A + B\,\mathrm{SST} = -4.0 \times 10^{-2} + 1.6 \times 10^{-3}\,\mathrm{SST}$, $D = I_o/c_p\rho_w$, $\beta = B\,L\rho_a C_D/c_p\rho_w$, and $T_o = (I_o/BL\rho_a C_D U) - (A/B) = \sim 28°$–$32°$C for reasonable I_o and U.

The correlations between the cloud forcing with SST and cloud forcing with $d\mathrm{SST}/dt$ are simply given by $-\cos\phi$ and $\sin\phi$, respectively. Analyzing the solution for two limiting cases in which the wind speed is held fixed, we can see that for very large H, or very short time scales, the rate of change

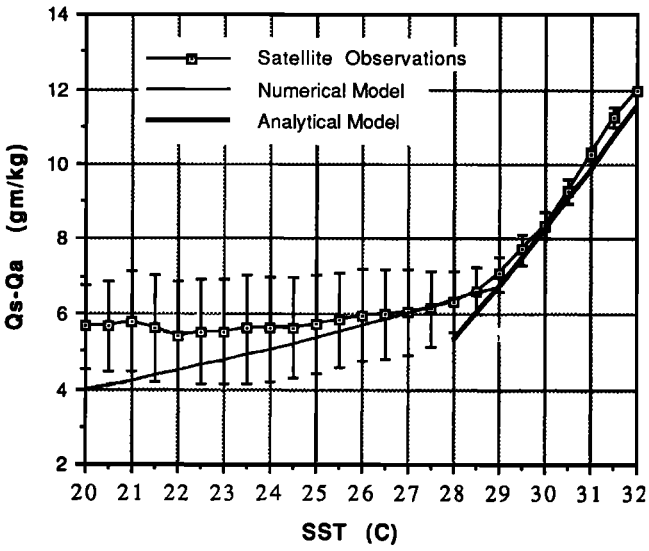

Fig. 4. Analytical model parameterization (thick solid line), satellite-derived monthly values (dotted line), and numerical model parameterization (thin solid line) (used in section 5) of Δq versus SST. Observed values are taken from the region 25°N to 25°S and 140°E to 170°W, over the years 1980–1985. Error bars denote standard deviations of the observed means. Note that analytical and numerical values of Δq overlap at SSTs >=29°C.

of SST is directly out of phase with the cloud forcing, and we would expect a strong negative correlation between cloud amount and dSST/dt. In the other limiting case of a very shallow mixed layer, or very long time scales, we would expect a strong negative correlation between cloud forcing and SST. Imposing a range of realistic values in the relationship for ϕ can yield either limit. For example, if U = 5 m s^{-1}, 5-day cloud fluctuations over a mixed-layer of 80-m results in a ϕ of about $-\pi/2$ (i.e., dSST/dt is highly correlated with contemporaneous cloud forcing and SST is not), while El Niño–Southern Oscillation time scale fluctuations (~4 years) over a mixed layer of 10 m results in a ϕ near zero (i.e., SST is highly correlated with contemporaneous cloud forcing and dSST/dt is not). Although the above system is highly idealized, it elucidates the difficulties in interpreting the correlations between SST and surface heating/cooling mechanisms (in this case "cloud" forcing) and highlights some of the gross physical parameters to be considered.

For the warm-pool region of the western tropical Pacific, typical mean wind speeds are 4 m s^{-1} [*Legler and O'Brien*, 1984], the mixed-layer depths are about 30 m (ranging between about 5–60 m; *Lukas and Lindstrom* [1991]), and most of the variability in convective activity at a given point is at time scales shorter than about 6 months [e.g., *Waliser et al.*, 1993]. Under such conditions, the simple model formulation above gives a value for ϕ of about $-\pi/3$. Thus assuming that the effects of other physical processes and measurement errors are not too large and that our convective indices are associated with decreases in surface solar radiation, observations (at high SSTs) from this region should indicate a relatively weak inverse relationship between convection and SST and a relatively strong inverse relationship between convection and dSST/dt. This suggestion is borne out by the plots in Figure 3 of convection versus SST (discussed previously) and the plots in Figure 5, which shows average anomalous rates of SST change (the annual cycle is removed) as a function of SST, and the two convection indices (Figures 5*a* and 5*b*) and their anomalies (Figures 5*c* and 5*d*). Figure 5 illustrates that diminished convection is associated with positive values of dSST/dt, and enhanced convection is associated with negative values of dSST/dt. This tendency is particularly strong for SSTs greater than or equal to 29°C. In this case, both HRC (Figures 5*a* and 5*c*) and OLR (Figures 5*b* and 5*d*) show the same qualitative behavior and approximately the same quantitative extreme (average) values of about ±0.1°C per month (student t tests at the 95% level indicate that these extreme values are significant relative to each other).

The results presented in this section demonstrate that organized convection, as measured by the HRC and OLR, acts locally to limit upward excursions of SST and that in general the presence of very warm SSTs (>~30°C) is, to some degree, a consequence of low or diminished amounts of local organized convection. Further, we have presented evidence to suggest that temporal correlations between SST and deep convection (or cloud processes) may be difficult to interpret. This difficulty arises for two reasons. The first reason stems from the character of the SST-convection relationship depicted in Figures 1 and 3 which show positive correlations between SST and convection for SSTs less than about 29°C, and low or even negative correlation for SSTs greater than about 30°C. Thus in regions where the "equilibrium" SST is about 29°–30°C, such as the western Pacific, little or no temporal (linear) correlation will be evident between time series of SST and convection. However, given their physical association and the evidence presented above, this cannot be interpreted as an indication that these two quantities are uncoupled, rather that they exhibit an important two-way coupling. The second reason that temporal correlations are difficult to interpret is that depending on the climatological characteristics of the region and the time scales of interest, the more apparent relation may be between deep convection and dSST/dt, rather than deep convection and SST, as was discussed above.

4. Interpretation

We hypothesize that the shapes of the convection proxy curves in Figures 1 and 3, and the relationships of dSST/dt versus SST and convection shown in Figure 5, result largely from three interacting processes operating within the coupled ocean-atmosphere system:

1. As SSTs increase (e.g., due to clear-sky surface insolation), the atmospheric column is destabilized, and the potential for organized convection increases.
2. Increases in organized convection result in decreased surface insolation due to clouds and increased vertical overturning, both of which cool the surface and increase the stability of the atmospheric column.
3. Internally generated atmospheric variability will result in spatial and temporal fluctuations in convection even if SSTs are temporally fixed and spatially homogeneous.

If only the first two processes above were active, an "equilibrium" state would be reached defined by a particular SST and intensity of convection. However, the third process prevents this equilibrium from being maintained, particularly on short time scales. Using the analogy of a "thermostat," the convective thermostat (in this case) is an imperfect one subject to random perturbations which forces the SST and

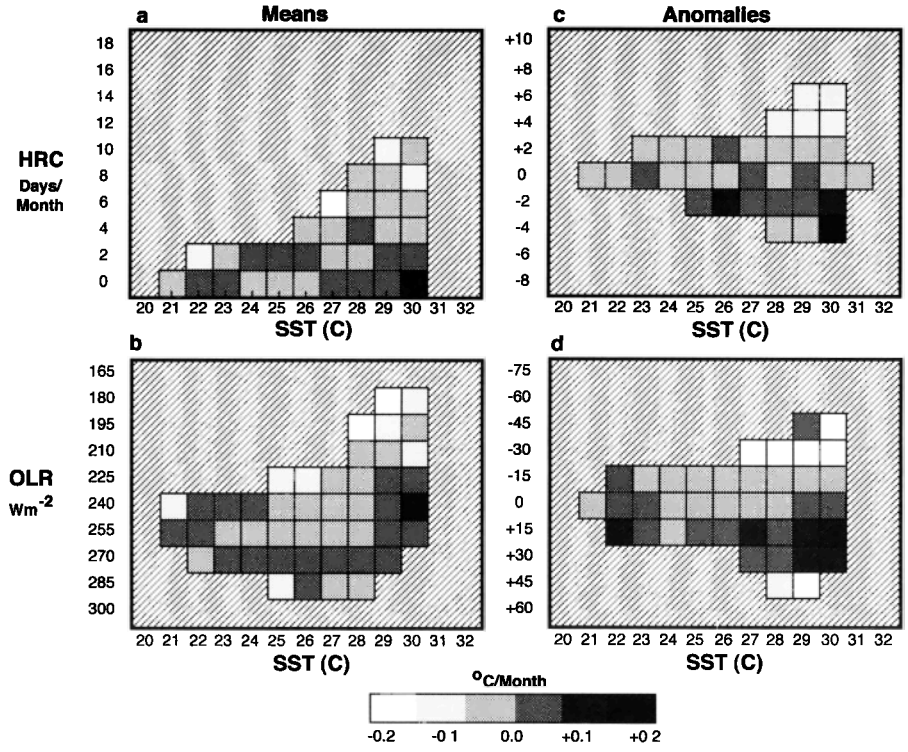

Fig. 5. Bin-averaged anomalous dSST/dt as a function of SST and (a) and (c) HRC and (b) and (d) OLR for the region 25°N to 25°S and 140°E to 170°W. Plots on the left are for monthly HRC and OLR totals. Plots on the right are for monthly HRC and OLR anomalies. All anomalies are computed about the annual cycle. Striped areas indicate bins with less than 50 observations.

convection to fluctuate about what would otherwise be their "equilibrium" values. We emphasize that the above conceptualization of the coupled system, including its more formal specification in the following section, is only relevant to times or regions where the influence of ocean dynamical processes on the evolution of SSTs is relatively small, and where SSTs are climatologically high enough to support convection, for example, the warm-pool region of the western tropical Pacific.

The first of the processes, described briefly above, is essentially the radiative component of a radiative-convective equilibrium. Surface warming due to clear-sky solar insolation results in increased moist static energy in the boundary layer due to enhanced SST-dependent latent and sensible heat fluxes out of the ocean. This heating and moistening of the lower levels, combined with radiative heat loss to space at higher levels, act to decrease the stability of the troposphere relative to the onset of moist convection.

The second of the above three processes is essentially the convective component of a radiative-convective equilibrium which develops to stabilize the system by transferring heat and moisture out of the boundary layer into the upper atmosphere. This vertical exchange is a complex process resulting in the generation of considerable cloud cover and the turbulent overturning of warm, moist air from lower levels with dry, cool air from upper levels (via convective and mesoscale updrafts and downdrafts [*Leary and Houze*, 1979; *Houze*, 1989]). Both the cloud cover, which diminishes surface solar radiation, and the vertical overturning, which allows the ocean to lose additional moist energy to the (locally) drier and cooler boundary layer by way of evaporative and sensible heat fluxes, function to decrease SST. However, the disparity between, and uncertainty concerning, the spatial and temporal scales over which these processes act can cause difficulties in determining which process is more important and for what time and space scales. Some of these difficulties are discussed below.

The third process involves the spatial and temporal organization of deep convection by tropical elements of the large-scale circulation such as the Hadley and Walker circulations [e.g., *Bjerknes*, 1966, 1969; *Schneider and Lindzen*, 1977], 30–60 day variability [e.g., *Madden and Julian*, 1972; *Lau and Chan*, 1988], and high-frequency tropical wave disturbances [e.g., *Yanai et al.*, 1968; *Wallace*, 1971]. Such organization influences the stability (i.e., temperature and moisture profiles) of the tropical atmosphere through (1) the local convergence or divergence of heat and moisture in the atmospheric boundary layer, particularly for the cases of intraseasonal and high-frequency variability, and (2) the large-scale transport of, moisture into, and latent heat out of, regions where convection is common, particularly in the cases of the Hadley and Walker circulations. These modulations in the atmospheric stability produce significant enhancements or reductions in the local convection that is independent of the local SST forcing. Thus to the local environment, this "organization" appears as a random forcing which inhibits the establishment of a local equilibrium between SST and convection. While we have emphasized the interactions between three processes on a local level, the influence of the large-scale circulations, particularly the transport of heat and moisture by the Hadley and Walker circulations, is the central reason why the first two processes

depart from components of true radiative-convective equilibrium.

As mentioned above, the cooling processes associated with convection include the diminished solar insolation at the surface due to the generated cloud systems and the modulation of surface heat fluxes due to the vertical overturning in the troposphere. Because useful measurements of both of these processes can be difficult to obtain and are relatively scarce and because the relative magnitudes of their effect is important in determining the character of the conceptual coupled system outlined above, we discuss some of these measurements and their implications below.

With respect to the effect on surface insolation due to clouds associated with deep convection, both satellite [e.g., *Liu and Gautier*, 1990; *Chertock et al.*, 1991; *Ramanathan and Collins*, 1991] and in situ measurements provide convincing evidence that such cloud forcing is significant. For example, Figure 6 shows the relationship between 5-day HRC and OLR anomalies versus in situ surface insolation anomalies from the American Samoa, an island located at the southeastern edge of the western Pacific warm pool. Both plots clearly show that large-scale convection, as measured by these indices, acts to diminish surface insolation, with reductions of up to 75 Wm^{-2} over 5-day time periods of intense convective activity. Thus the cloud systems associated with organized deep convection, as measured by OLR and HRC indices, do produce important systematic reductions is surface solar radiation. Similarly, *Young et al.* [1992] examined the differences between surface solar flux in disturbed and undisturbed weather gathered on a research cruise in the western tropical Pacific and report average reductions in local insolation under disturbed conditions of approximately 24% (46 Wm^{-2}).

With respect to the relation between organized convection and the surface fluxes of heat and moisture, the in situ measurements of *Young et al.* [1992] show local increases in average turbulent fluxes associated with convective disturbances of the order of 10%, approximately 10 Wm^{-2} (20% increase in sensible flux (2.3 Wm^{-2}), 6% increase in latent flux (6.6 Wm^{-2})). Similar tendencies were reported from the GATE experiment [e.g., *Gaynor and Ropelewski*, 1979; *Johnson*, 1981]. These enhancements arise partly through increased gradients of temperature and moisture between the surface and the boundary layer, and partly through enhanced, highly transient, low-level winds, both of which arise from turbulent activity of convection. Given these findings, one might expect regions of frequent convective activity, such as the western Pacific, to be local evaporation and sensible heat flux maxima. However, large-scale climatological observations derived from ship reports indicate that such regions are actually local minima [*Weare et al.*, 1980].

To indicate how such contradictory behavior between the local and large-scale tendencies of evaporative flux might come about, we examine relationships between organized convection and quantities important to the parameterization of evaporative heat flux (see equation (1)). Figure 7 illustrates the influence of convection anomalies on Δq (Figure 7*a*) and surface wind speed (Figure 7*b*) anomalies using data from the western tropical Pacific. These plots have been divided into strongly and weakly convective regimes. For both weak and strong convection regimes, Δq decreases with increasing convection, implying that increases in organized convection are associated with decreases in evaporative flux. This result is in contrast to the local studies referenced above [*Leary and Houze*, 1979; *Houze*, 1989; *Young et al.*, 1992; *Gaynor and Ropelewski*, 1979; *Johnson*, 1981], where turbulent vertical exchange (i.e., saturated updrafts and unsaturated downdrafts) acts to increase Δq and thus evaporation. However, such a tendency for large-scale Δq (Figure 7*a*) is consistent with the fact that organized convection is closely tied to low-level horizontal convergence of moisture, and enhanced large-scale moisture convergence implies an increase in the large-scale q_a. These increases in q_a result in a decrease in large-scale Δq and thus a decrease in evaporation [cf. *Liu and Gautier*, 1990; *Betts and Ridgway*, 1989]. Applying the bulk formula for evaporation (see equation (1)) with typical values for C_D and ρ_a, and assuming a mean wind speed of about 5 m s^{-1}, the Δq

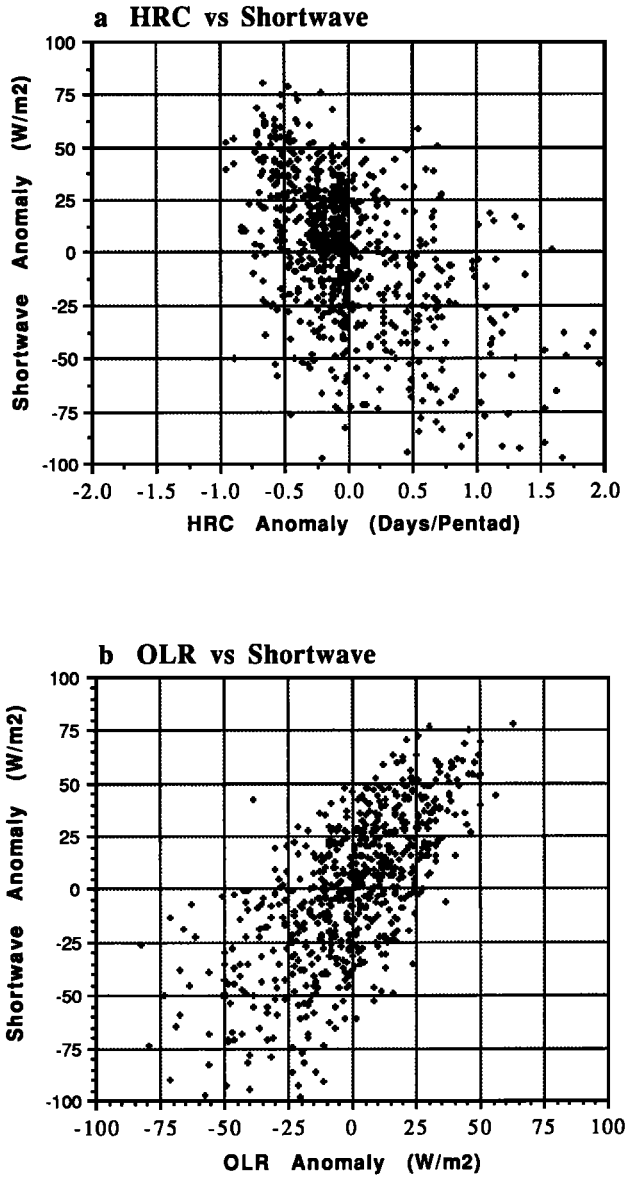

Fig. 6. Five-day average anomaly values of surface-measured solar irradiance at American Samoa (14.3°S, 170.6°W) plotted against 5-day values of (*a*) HRC and (*b*) OLR anomalies between the years 1976 and 1987. Anomalies are taken about the annual cycle.

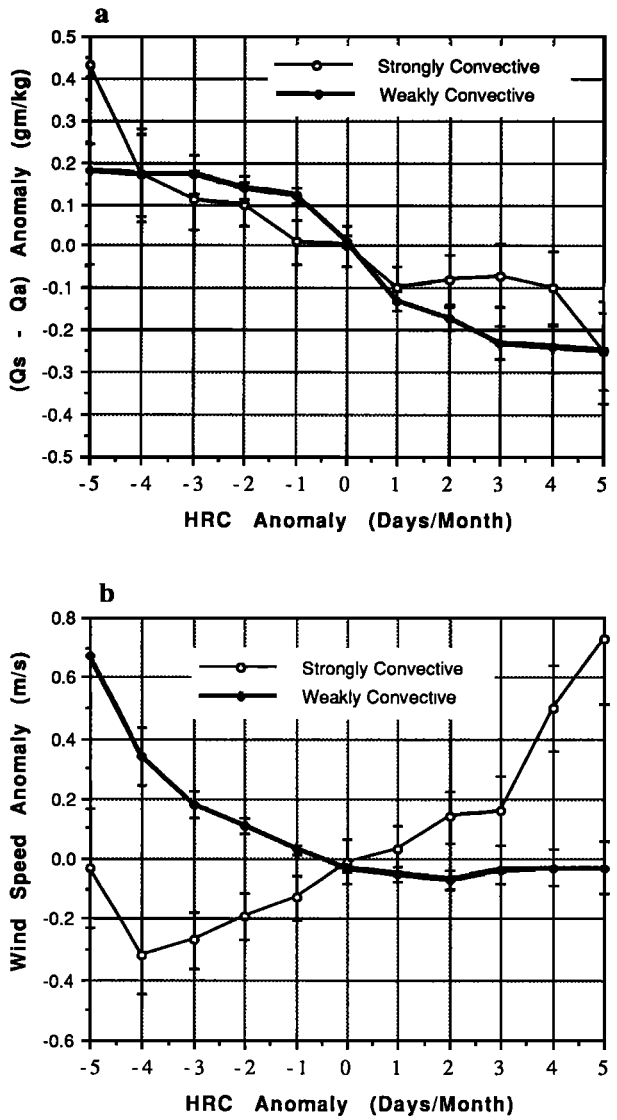

Fig. 7. Anomalous monthly (*a*) Δq and (*b*) wind speed versus anomalous monthly HRC for the region 25°N to 25°S and 140°E to 170°W. Anomalies are computed about the annual cycle (*a*) for the years 1980–1985 for Δq and (*b*) 1975–1987 for wind speed. Thick (thin) lines indicates values were used only from regions, where the mean annual cycle of HRC is less (greater) than 5 days/month. Error bars denote 95% confidence interval for bin means estimated by the student *t* test.

anomalies in Figure 7*a* amount to evaporation anomalies of about ± 5 Wm^{-2}.

The relationships between anomalies in convection and wind speed shown in Figure 7*b* are more complex than those for Δq. The plot for weakly convecting regions tends to reflect the overall tendency for mean surface wind speed to decrease with mean convection amount [*Legler and O'Brien*, 1984; *Waliser et al.*, 1993] due most likely to wind field becoming more convergent. Thus these data suggest that in such regions, periods of increased convection are associated with decreased evaporative fluxes. The plot for strongly convecting regions, however, indicates the opposite trend between surface winds and anomalies in convection. Because mean wind speeds are low (~4 m s^{-1}) in these regions, local increases in boundary layer wind speeds due to convective disturbances, such as those found by *Young et al.* [1992] are more likely to produce detectable increases in the (larger-scale) monthly mean wind speed observations. Again, applying the bulk formula for evaporation, and assuming a mean Δq of about 8 g kg^{-1}, the wind speed anomalies in Figure 7*b* amount to about ± 15 W m^{-2}. If the relative decreases in Δq (with increased convection, Figure 7*a*) are smaller than the relative increases in the surface winds, then increases in evaporative fluxes would possibly result; for the data used to prepare Figure 7, the changes in wind and Δq approximately balanced (± 5 W m^{-2}) when all eddy terms were taken into account.

The above results are presented to demonstrate that the relationship between convection and the surface fluxes of latent and sensible heat appears to be scale dependent but has yet to be well defined. Nevertheless, the recent in situ measurements by *Young et al.* [1992] and the large-scale relationships presented in this paper, suggest that the effect on solar radiation from cloud cover related to organized convection is considerably larger than that related to systematic increases in turbulent surface fluxes. The recently completed *TOGA COARE* [1991] experiment is designed in part to address these important issues and determine more completely the influence of convection on the surface energy fluxes of the warm-pool regions of the tropics.

5. Simplified Model Analysis

To demonstrate that the three elements of the idealized system described above can interact to qualitatively reproduce the observed relationships between SST and convection examined in section 3, we have incorporated them into a simple, time-dependent coupled ocean-atmosphere model. The general description of the model is presented below with some of the parameterization details given in the appendix.

The evolution of the model SST is formulated as

$$\frac{d\mathrm{SST}}{dt} = \frac{1}{c_p \rho_w H}\{Q_{S0}(1 - C) - Q_E - Q_L - Q_S\}. \quad (3)$$

Q_{S0} is the clear sky surface insolation. This quantity is calculated for each day of the year from daily averaged solar radiation values at the top of the atmosphere with reductions for scattering, absorption, and ocean albedo (see appendix, model specification 1). As model integrations proceed, the latitude is stepped from 24° to the equator at 2° increments to achieve a representative sampling of the solar conditions represented in the observations. The variable C represents the fraction of incoming solar radiation reflected by the cloud systems associated with organized convection. Its value is determined as follows. First, at each model time step (1 day), a "potential convection" amount (Pc) is calculated as

$$\mathrm{Pc} = 0.0; \ \mathrm{SST} <= 25°\mathrm{C}$$

$$\mathrm{Pc} = 0.3; \ \mathrm{SST} >= 29.5°\mathrm{C} \quad (4)$$

$$\mathrm{Pc} = 0.3*((\mathrm{SST} - 25)/4.5)^3 \quad \text{otherwise}$$

This relation is designed to qualitatively represent the first process described in the previous section; that is, in the absence of other factors, the ability of the atmosphere to support organized convection increases sharply with SST at temperatures above approximately 26°C, with increases in SST appearing to have less effect on the development of

convection when SST is above about 29°C (for example, *Graham and Barnett* [1987], and Figures 1 and 3). The upper limit of 0.3 was chosen to roughly correspond to the facts that in warm tropical areas mean monthly values of HRC are about 10 days/month [*Garcia*, 1985; *Waliser and Gautier*, 1993], and (2) estimates of albedo about 30% [*Liou*, 1980]. Note that because our emphasis is to simulate the behavior of the actual coupled system at the highest SSTs, the treatment of the model in this lower SST range can be adequately represented by this (or any similar) empirical relation, for example, a linear one.

Added to this "potential convection" is a stochastic component (Rc) representing the time varying influences of the large-scale circulation (that is, the third process described in the previous section). Rc is calculated from an autoregressive process, having temporal statistics similar to those of the HRC data over the western tropical Pacific (see appendix, model specification 2); in agreement with the behavior of observed convective indices, the magnitude of the stochastic component increases with SST (linearly in the model), up to 29.5°C. The actual model convective index is the sum of the "potential convection" and the stochastic component (i.e., $C = \mathrm{Pc} + Rc$), with the constraint that no more than 60% of the incoming solar radiation is reflected on a given day. Thus the term $(1 - C)$ represents the reduction in surface solar radiation due to organized convective cloud systems (that is, the solar component of the second process outlined in the previous section).

The net longwave radiation flux at the ocean surface (Q_L) is parameterized as

$$Q_L = (0.94(\sigma)\mathrm{SST}^4) - [-2800.0 + (\mathrm{SST})10.64] \quad (5)$$

where the first term on the right is the Stefan-Boltzmann relation for outgoing flux, and the second term is an empirical fit that provides values consistent with the recent net surface longwave flux calculations of *Kiehl and Briegleb* [1992]. These measurements reflect an explicit greenhouse effect resulting in decreased net longwave flux, as SSTs increase.

Q_E and Q_S are bulk parameterizations of latent and sensible heat flux (see appendix, model specification 3):

$$Q_E = L\rho_a C_D U\ \Delta q \qquad \Delta q = q_w(\mathrm{SST}) - q_a(T_a, Rh) \quad (6)$$

$$Q_S = \rho_a C_D U\ \Delta T \qquad \Delta T = \mathrm{SST} - T_a. \quad (7)$$

In these formulations, the air temperature (T_a) is an especially important term, mainly because it enters into the calculation of the near-surface specific humidity (q_a) for the latent heat flux. We use the relation

$$\begin{aligned} T_a &= \mathrm{SST} - 1.5°\mathrm{C} \qquad \mathrm{SST} < 29°\mathrm{C} \\ T_a &= 27.5°\mathrm{C} \qquad \mathrm{SST} >= 29°\mathrm{C} \end{aligned} \quad (8)$$

which is consistent with in situ observations in that the sea-air temperature difference increases rapidly with SST at SSTs above about 29°C [e.g., *Weare et al.*, 1980]. Using this relation, we calculate near-surface specific humidity as

$$q_a(T_a, \mathrm{Rh}) = \mathrm{Rh}^* q_s(T_a) \quad (9)$$

where $q_s(T_a)$ is the saturation-specific humidity at T_a and the relative humidity (Rh) is assigned a value of 80%. Figure 4 shows that the above relationship yields values of Δq that agree well with observations from the region of the western Pacific. The close fit between the satellite-inferred and parameterized values of Δq at high SSTs suggest that ventilation with drier air from cooler regions poleward and eastward via the Hadley and Walker circulations is an important process governing the heat budget of the warm-pool regions. Note that the important aspect of equations (8) and (9) is that they give good estimates of $q_a(T_a, \mathrm{Rh})$ over the range of SST, and region, of interest; the actual value of T_a used in the calculation of the sensible heat flux has little impact on model behavior (see appendix, model specification 4). The wind speed for the model was calculated using an autoregressive lognormal distribution with statistics similar to those observed (see appendix, model specification 5).

As discussed earlier, consistent with the characterization of organized convection as a process of vertical overturning, resulting in the mixing of cooler, drier air from the upper troposphere into the boundary layer, there is observational evidence that the local fluxes of latent and sensible heat tend to be increased during episodes of convection [e.g., *Young et al.*, 1992; *Gaynor and Ropelewski*, 1979; *Johnson*, 1981]. This "coupling" between the turbulent heat fluxes and organized convection (i.e., the surface flux component of the second process outlined in the previous section) was incorporated into the model by modulating the values of Q_E and Q_S as a function of the level of model "convection" (i.e., according to the value of C and in the same manner as done for Q_{S0}) so that the percentage differences in these terms between highly convective and modestly convective agreed approximately with the values given by Young et al. Sensitivity tests showed that this coupling has little effect on the behavior of the model, even when the percentage increases in flux were multiplied by a factor of 4.

The depth of the ocean "mixed layer" was fixed at 30 m, in close agreement with the measurements from the western tropical Pacific [*Lukas and Lindstrom*, 1991], where the model physics are most applicable. These data showed that although the top of the main thermocline is typically located at depths of 50 m to 100 m, the depth of the effective mixed layer is reduced to an average value of 29 m by stratification due to the presence of less saline near-surface water produced by precipitation associated with convection.

The model was integrated over a period long enough to provide approximately the same number of monthly average SST and convection "observations" as in Figures 1*a*, 1*b*, and 3. Figure 8*a* shows the simulated relationships between model convection C, SST, and SST population-binned as in Figure 1 for the model in its "standard" configuration (i.e., with convective cloud effects and convection-surface heat flux coupling), and from an otherwise identical integration in which it is assumed that the model "clouds" are transparent to solar radiation. In the standard configuration, both the convective index and SST population curves are quite similar to those seen in observations. With respect to the role of convective clouds in regulating warm-pool SSTs, the most important points of agreement are the fact that the peak of the population curve is at approximately the correct point and drops steeply at higher temperatures, and that the highest SSTs are associated with diminished amounts of convection. (As noted, the ascending branch of the convective index curve is "built in" to the model, so agreement with observations here is expected.) These points of agree-

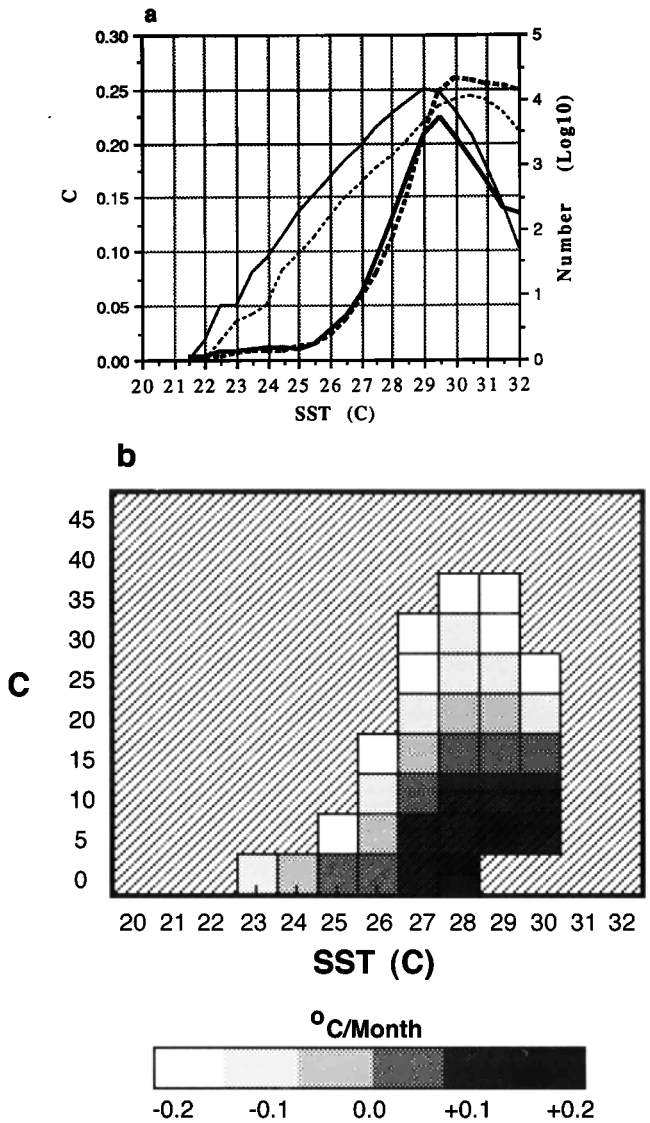

Fig. 8. (*a*) Same as Figures 1*a* and 1*b* except using model "convection" C (see text for description). Solid lines denote simulation with standard physics, dashed lines denote simulation with "transparent" clouds. Thin solid lines denote SST population, thick solid lines denote model value of C. (*b*) Same as Figures 5*a* and 5*b* except using model "convection" C.

ment between observations and the behavior of this simple surface energy balance model, together with the strong evidence for important reductions in surface insolation by convective clouds (e.g., Figure 6), suggests that the conceptual framework of the model is correct; that is, the reduction in surface insolation by the clouds associated with organized convection does assist in regulating warm pool SSTs.

To get a qualitative estimate of how large a role convective cloud systems play in determining the character of warm-pool SSTs, a second population curve in Figure 8*a* shows the model's behavior in an identical simulation but in which the "clouds" are assumed to be transparent. It can be seen that without the reduction in solar radiation by convective clouds the peak of the population curve is found at 31°C, about 1.5°C warmer than with the cloud shielding effect. Perhaps more impressive is the fact that without the shortwave absorption by clouds, rarely observed SSTs of 32°C or more would be significantly more common. An additional point made by these curves is that turbulent (primarily latent) fluxes are the only mechanisms remaining to constrain upward excursions of SST [*Newell*, 1979]; the effect of convective clouds is to shift the entire distribution toward cooler temperatures by 1°–2°C [*Graham and Barnett*, 1987].

Figure 8*b* shows bin-averaged rates of simulated SST change as a function of SST and convective cloud albedo. The distribution is very similar to the analogous plots using observations shown in Figure 5. In the range of high SSTs in particular, "above average" amounts of convection are associated with surface cooling of about 0.2°C/month and "below average" amounts are associated with surface warming of about 0.2°C/month surface warming. The fact that these simulated values are about twice those calculated from the observations may reflect the influence of processes neglected in the model such as horizontal advection and vertical mixing in the upper ocean, or the fact that the HRC and OLR are only proxies to convection and thus are not the "pure" measures of convection nor albedo available from the model (i.e., they are not direct measures of surface heat flux; Wm^{-2}). Although the above model is highly idealized, it helps to illustrate that given a realistic specification of model parameters, the interaction between the three processes described in the previous section does qualitatively reproduce basic aspects of the observed relationships between deep convection and SST that are not reproduced without the effect of convective clouds on surface solar radiation. Further, sensitivity studies on model parameters such as wind speed, mixed-layer depth, wind speed and convection statistics, imposed value of Q_{SO}, etc., showed that the model results were qualitatively insensitive to reasonable changes in their values.

6. Discussion

The results and ideas presented above are in agreement with, and extend, some earlier considerations regarding this topic. *Newell* [1979] considered the equilibrium tropical oceanic surface heat budget under typical meteorological conditions for regions where deep convection is common. These idealized calculations showed that under cloud-free conditions, the outgoing surface fluxes (sensible, latent, longwave) balance the incoming solar radiation at an SST of about 30°–31°C. Further, at temperatures of about 32°–33°C, the heat losses, which are dominated by the evaporative term, far exceed the solar input. This led Newell to suggest that latent heat flux places a "natural" limit on SSTs. These "predicted" maximum temperatures are near the observed (although rarely occurring) maximum SSTs for both monthly and long-period averages, and as shown in Figure 1, tend to occur under relatively cloud-free skies. On the basis of Newell's calculations and observations such as those in Figure 1*b*, *Graham and Barnett* [1987] suggested that the reason that the observed "equilibrium" temperature (taken as the maximum of the SST population curve) appears to be near 28.0°C is that the reduction in surface solar radiation by clouds associated with organized convection. On the basis of their "thermostat" hypothesis of SSTs being limited by the solar shielding effects of thick cirrus clouds and observed values of radiative feedbacks, *Ramanathan and Collins* [1991] calculated upper limits on SST of about 29°–32°C.

The observational evidence presented in this paper sug-

gests that the upper limit of long-term monthly average SSTs in a regime of deep convection is about 29.5°C with higher surface temperatures associated with, and resulting from, decreasing convection. Thus while evaporative heat flux may place a "natural" limit on SSTs of about 32°C (as suggested by *Newell* [1979]), the cooling mechanisms associated with organized convection, particularly cloud cover, result in an observed limit on SSTs of about 30°C (for monthly and longer time scales). It must be emphasized, that the vertical exchange processes associated with large-scale deep convection strongly influence the choice of the typical meteorological conditions used in calculations such as Newell's (e.g., surface air temperature and relative humidity). Thus the clear-sky SST limit obtained from such calculations are better viewed from the perspective of occurring in an environment with organized convection but transparent clouds, than one in which organized convection is absent. It should be emphasized that these "limits" are relevant only to the present-day climate, and it seems likely that under a scenario of increased greenhouse gas concentrations, the processes described here would operate in a similar manner but that the SST population distribution would be shifted towards warmer SSTs.

As a final point concerning our understanding of the climate system and climate change, consider the relationships between organized deep convection and SST inferred by two tropical modelers, one using an atmospheric model forced with observed SSTs, the other using an ocean model forced with observed atmospheric fluxes of heat and radiation. Given current parameterizations of large-scale deep convection, the atmospheric modeler will probably infer that convection tends to occur most frequently and intensely over the warmest water. On the other hand, the ocean modeler will find (assuming homogeneous dynamical conditions) that the warmest SSTs occur under clear or nonconvective skies. In conclusion, this contrast emphasizes the inadequacy of studying the Earth's climate, especially the relationship between organized deep convection and SST, in an uncoupled framework.

APPENDIX: MODEL SPECIFICATIONS

1. $Q_{S0} = I_o(\phi, t)$ (1-scattering) (1-absorption) (1-albedo); I_o is top of the atmosphere solar insolation as a function of latitude and season, scattering is 0.08, absorption is 0.22, and albedo is 0.06 [*Liou*, 1980; *Payne*, 1972].

2. E-folding time of C is 14 days (due mostly to autocorrelation of Pc = F(SST)]; mean is 0.14; standard deviation is 0.15; max is 0.6 (about 1.2% of cases); min is 0.0 (about 30% of cases); mode is 0.08; E-folding time of random signal is 3 days (and about ~0.2 at 30 days). In some experiments a small additional component (with amplitude 20% of the random component) was added to Rc to simulate 40–60 day variability. Although this considerably altered the autocorrelation structure of Rc, it produced little effect on the behavior of the model.

3. The value of the drag coefficient was set at 0.0015.

4. For example, the model was integrated using (8) to calculate Δq, but using a fixed air-sea temperature difference (1.5°C) in the sensible flux calculation.

5. Daily wind speed statistics: E-folding time of 8 days; mean is 5.1; standard deviation is 1.69; max is 14.6; min is 2.6; mode is 4.9 m/s.

Acknowledgments. We thank Catherine Gautier, Dan Cayan, and Richard Somerville for useful suggestions and comments regarding the manuscript. We would also like to thank the two reviewers for their suggestions and comments. The first author would like to thank Roberto Mechoso and David Neelin for sponsoring the continuation and completion of this work. This research was supported in part by the California Space Institute under mini-grant CS 45-90 (DW), by the UCAR sponsored NOAA Climate and Global Change Postdoctoral Fellowship program (DW), by NSF under grant ATM89-11592 (NG), by NOAA under grant NA86AA-D-CP104 for the Experimental Climate Forecast Center at the Scripps Institution of Oceanography (NG), and by a grant from the G. Unger Vetlesen Foundation to the Scripps Institution of Oceanography (NG), and by the University of California and Digital Equipment Corporation under grant 1243. A portion of the illustration utilized software developed by the National Center for Supercomputing Applications at the University of Illinois at Urbana-Champaign.

REFERENCES

Arking, A., The radiative effects of clouds and their impact on climate, *Bull. Am. Meteorol. Soc.*, *71*, 795–813, 1991.

Betts, A. K., and W. Ridgway, Climatic equilibrium of the atmospheric convective boundary layer over a tropical ocean, *J. Atmos. Sci.*, *46*, 2621–2641, 1989.

Bjerknes, J., A possible response of the atmospheric Hadley circulation to equatorial anomalies of ocean temperature, *Tellus*, *18*, 820–829, 1966.

Bjerknes, J., Atmospheric teleconnections from the equatorial Pacific, *Mon. Weather Rev.*, *97*, 163–172, 1969.

Chelliah, M., and P. Arkin, Large-scale interannual variability of monthly outgoing longwave radiation anomalies over the global oceans, *J. Climate*, *5*, 371–389, 1992.

Chertock, B., R. Frouin, R. C. J. Somerville, Global monitoring of net solar irradiance at the ocean surface: Climatological variability and the 1982–83 El Nino, *J. Climate*, *4*, 639–650, 1991.

Dutton, E., NOAA climate monitoring and diagnostics laboratory, Data obtained from the GEDEX CD-ROM, NASA Goddard Space Flight Center, Greenbelt, Md., 1992.

Fu, R., A. D. Del Genio, W. B. Rossow, and W. T. Liu, Cirrus-cloud thermostat for tropical sea surface temperatures tested using satellite data, *Nature*, *358*, 394–397, 1992.

Gadgil, S., P. V. Joseph, and N. V. Joshi, Ocean-atmosphere coupling over monsoon regions, *Nature*, *312*, 141–143, 1984.

Gadgil, S., A. Guruprasad, and J. Srinivasan, Systematic bias in the NOAA outgoing longwave radiation dataset, *J. Climate*, *5*, 867–875, 1992.

Garcia, O., Atlas of Highly Reflective Clouds for the Global Tropics: 1971–1983, *U.S. Dep. of Commerce, NOAA*, Environmental Research Lab., Boulder, Colo., 1985.

Gaynor, J. E., and C. F. Ropelewski, Analysis of the convectively modified GATE boundary layer using in-situ and acoustic sounder data, *Mon. Weather Rev.*, *107*, 985–993, 1979.

Graham, N. E., and T. P. Barnett, Sea surface temperature, surface wind divergence, and convection over tropical oceans, *Science*, *238*, 657–659, 1987.

Gruber, A., and A. F. Krueger, The Status of the NOAA Outgoing Longwave Radiation Data Set, *Bull. Am. Meteorol. Soc.*, *65*, 958–962, 1984.

Horel, J., and A. G. Cornejo-Garrido, Convection along the coast of northern Peru during 1986: Spatial and temporal variation of clouds and rainfall, *Mon. Weather Rev.*, *114*, 2091–2105, 1986.

Houze Jr., R. A., Observed structure of mesoscale convective systems and implications for large-scale heating, *Q. J. R. Meteorol. Soc.*, *115*, 425–461, 1989.

Johnson, R. H., Large-scale effects of deep convection on the GATE tropical boundary layer, *J. Atmos. Sci.*, *111*, 2399–2413, 1981.

Kiehl, J. T., and B. P. Briegleb, Comparison of the observed and calculated clear sky greenhouse effect: Implications for climate studies, *J. Geophys. Res.*, *97*, 10,037–10,049, 1992.

Krueger, A. F., and T. I. Gray, Jr., Long-term variations in equatorial circulation and rainfall, *Mon. Weather Rev.*, *97*, 700–711, 1969.

Lau, K. M., and P. H. Chan, Intraseasonal and interannual varia-

tions of tropical convection: A possible link between the 40–50 day oscillation and ENSO?, *J. Atmos. Sci.*, *45*, 506–521, 1988.
Lau, K. M., and S. Shen, On the dynamics of intraseasonal oscillations and ENSO, *J. Atmos. Sci.*, *45*, 1781–1797, 1988.
Leary, C. A., and R. A. Houze, Jr., The structure and evolution of convection in a tropical cloud cluster, *J. Atmos. Sci.*, *36*, 437–457, 1979.
Legler, D. M., and J. J. O'Brien, Atlas of tropical pacific wind stress climatology 1971–1980, Dep. of Meteorol., Florida State Univ., Tallahassee, Fla., 1984.
Liebmann, B., and D. L. Hartmann, Interannual variations of outgoing IR associated with tropical circulation changes during 1974–1978, *J. Atmos. Sci.*, *39*, 1153–1162, 1982.
Lindzen, R. S., Some coolness concerning global warming, *Bull. Am. Meteorol. Soc.*, *71*, 288–299, 1990.
Lindzen, R. S., and S. Nigam, On the role of sea surface temperature gradients in forcing low-level winds and convergence in the tropics, *J. Atmos. Sci.*, *44*, 2418–2436, 1987.
Liou, K. N., *An Introduction to Atmospheric Radiation*, Academic, San Diego, Calif., 1980.
Liou, K., Influence of cirrus clouds on weather and climate processes: A global perspective, *Mon. Weather Rev.*, *114*, 1167–1199, 1986.
Liu, W. T., Statistical relation between monthly mean precipitable water and surface-level humidity over global oceans, *Mon. Weather Rev.*, *114*, 1591–1602, 1986.
Liu, W. T., The annual and interannual variabilities of precipitable water, surface wind speed, and sea surface temperature over the tropical pacific, *Ocean-Air Interactions*, *1*, 195–219, 1989.
Liu, W. T., and C. Gautier, Thermal forcing on the tropical pacific from satellite data, *J. Geophys. Res.*, *95*, 13,209–13,217, 1990.
Lukas, R., and E. Lindstrom, The mixed-layer of the western equatorial Pacific Ocean, *J. Geophys. Res.*, *96*, 3343–3357, 1991.
Madden, R., and P. Julian, Description of global scale circulation cells in the tropics with a 40–50 day period, *J. Atmos. Sci.*, *29*, 1109–1123, 1972.
Manabe, S., and R. T. Weatherald, Thermal equilibrium of the atmosphere with a given distribution of relative humidity, *J. Atmos. Sci.*, *24*, 241–259, 1967.
Neelin, J. D., and I. M. Held, Modeling tropical convergence based on moist static energy budget, *Mon. Weather Rev.*, *115*, 3–12, 1987.
Newell, R. E., Climate and the ocean, *Am. Sci.*, *67*, 405–416, 1979.
Paltridge, G. W., Cloud-radiation feedback to climate, *Q. J. R. Meteorol. Soc.*, *106*, 895–899, 1980.
Payne, R. E., Albedo of the sea surface, *J. Atmos. Sci.*, *29*, 959–970, 1972.
Ramanathan, V., and J. A. Coakley, Jr., Climate modeling through radiative-convective models, *Rev. Geophys. Space Phys.*, *16*, 465–489, 1978.
Ramanathan, V., and W. Collins, Thermodynamic regulation of ocean warming by cirrus clouds deduced from observations of the 1987 El Nino, *Nature*, *351*, 27–32, 1991.
Ramanathan, V., and W. Collins, Thermostat and global warming, *Nature*, *357*, 649, 1992.
Rasmusson, E. M., and J. M. Wallace, Meteorological Aspects of the El Nino/Southern Oscillation, *Science*, *222*, 1195–1202, 1983.
Reynolds, R. W., A real-time global sea surface temperature analysis, *J. Climate*, *1*, 75–86, 1988.
Rossow, W. B., and R. A. Schiffer, ISCCP cloud data products, *Bull. Am. Meteorol. Soc.*, *72*, 2–20, 1991.
Schneider, E. K., and R. S. Lindzen, Axially symmetric steady-state for instability and climate studies, Part I, Linearized calculations, *J. Atmos. Sci.*, *34*, 263–279, 1977.
Somerville, R. C. J., and L. A. Remer, Cloud optical thickness feedbacks in the CO_2 climate problem, *J. Geophys. Res.*, *89*, 9668–9672, 1984.
Stephens, G. L., On the relationship between water vapor over the oceans and sea surface temperature, *J. Climate*, *3*, 634–645, 1990.
TOGA COARE, "Tropical Ocean Global Atmosphere: Coupled Ocean Atmosphere Response Experiment. Experiment Design," TOGA COARE Projects Office, University Corporation of Atmospheric Research, Boulder, Colo., 1991.
Waliser, D. E., and C. Gautier, A satellite-derived climatology of the ITCZ, *J. Climate*, in press, 1993.
Waliser, D. E., N. E. Graham, and C. Gautier, Comparison of the highly reflective cloud and outgoing longwave data sets for use in estimating tropical deep convection, *J. Climate*, *6*, 331–353, 1993.
Wallace, J. M., Spectral studies of tropospheric wave disturbances in the tropical western pacific, *Rev. Geophys.*, *9*, 557–611, 1971.
Wallace, J., Effect of deep convection on the regulation of tropical sea surface temperature, *Nature*, *357*, 230–231, 1992.
Weare, B. C., P. T. Strub, and M. D. Samuel, Marine climate atlas of the tropical Pacific Ocean, Dep. of Land, Air and Water Resources, University of California, Davis, 1980.
Webster, P. J., Response of the tropical atmosphere to local steady forcing, *Mon. Weather Rev.*, *100*, 518–541, 1972.
Yanai, M., T. Maruyama, T. Nitta and Y. Hayashi, Power spectra of large-scale disturbances of the tropical Pacific, *J. Meteorol. Soc. Jpn.*, *46*, 308–323, 1968.
Young, G. S., D. V. Ledvina, and C. W. Fairall, Influence of precipitating convection on the surface energy budget observed during a TOGA pilot cruise in the tropical western Pacific Ocean, *J. Geophys. Res.*, *97*, 9595–9603, 1992.
Zhang, C., Large-scale variability of atmospheric deep convection with respect to sea surface temperature in the tropics, *J. Clim.*, in press, 1993.

N. E. Graham, Climate Research Division, Scripps Institution of Oceanography, University of California, San Diego, La Jolla, CA 92093.

D. E. Waliser, Department of Atmospheric Sciences, University of California, Los Angeles, Los Angeles, CA 90024.

(Received November 9, 1992;
revised March 29, 1993;
accepted March 29, 1993.)